ACS APPLIED MATERIALS & INTERFACES

Research Article

www.acsami.org

Organic/Metallic Nanohybrids Based on Amphiphilic Dumbbell-Shaped Dendrimers

Shi-Min Shau,[†] Chia-Cheng Chang,[†] Chia-Hao Lo,[†] Yi-Chu Chen,[†] Tzong-Yuan Juang,[‡] Shenghong A. Dai,[†] Rong-Ho Lee,*[,†] and Ru-Jong Jeng*[,†,§]

[†]Department of Chemical Engineering, National Chung Hsing University, Taichung 402, Taiwan

[‡]Department of Applied Chemistry, National Chiayi University, Chiayi 60004, Taiwan

[§]Institute of Polymer Science and Engineering, National Taiwan University, Taipei 10617, Taiwan

Supporting Information

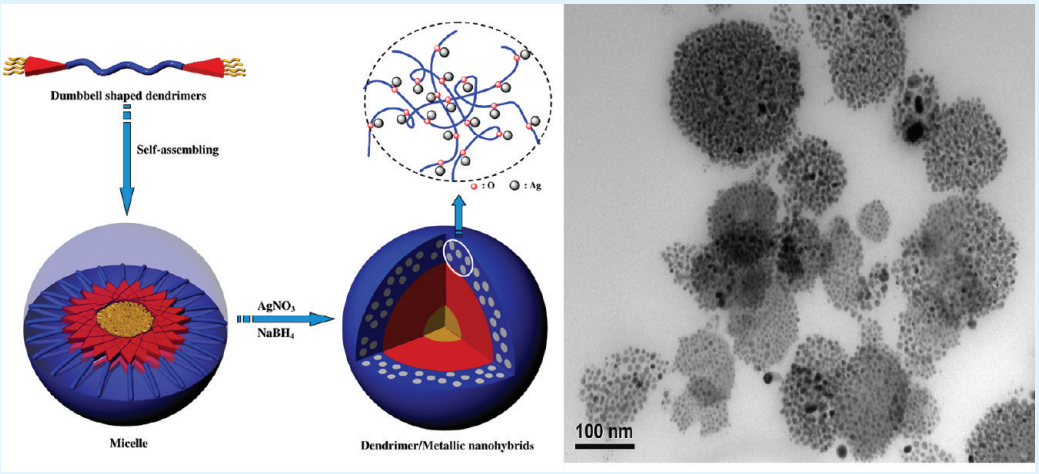

ABSTRACT: In this study, we synthesized a series of amphiphilic dumbbell-shaped dendrimers through the addition reactions of a hydrophilic poly(oxyalkylene) with hydrophobic dendrons based on 4-isocyanate-4′-(3,3-dimethyl-2,4-dioxo-azetidine)-diphenylmethane with different numbers of branching generations. The addition reaction of azetidine-2,4-diones of dendrons to amines of poly(oxyalkylene) was proceeded by stirring the reactants in dry tetrahydrofuran (THF) under nitrogen at 60 °C. In aqueous media, the dumbbell-shaped dendrimers self-assembled into micelles with their hydrophobic dendrons in the core and their hydrophilic poly(oxyalkylene) segments forming loops in the corona shell. Employing the unique self-assembled micelle structures as templates for subsequent chemical reduction of the Ag^+ ions, we generated new types of organic/metallic [silver nanoparticle (AgNP)] nanohybrid clusters. The long poly(oxyalkylene) loops that extended into the aqueous phase complexed with the Ag^+ ions, providing the suspension with steric stabilization to prevent the AgNPs from collision and flocculation. After reduction, the AgNPs were present in a homogeneous distribution in the round dendrimer micelle−stabilized nanoclusters. The diameter of each AgNP was less than 10 nm; the diameter of each round nanocluster was in the range of 50−200 nm. The encapsulation efficiency of the AgNPs in micelles was about 54−69% for the dumbbell-shaped dendrimer based organic/AgNP nanohybrid.

KEYWORDS: *dendron, dumbbell-shaped dendrimer, self-assembly, silver nanoparticle*

INTRODUCTION

The self-assembly of low-molecular-weight amphiphiles,[1] linear block copolymers,[2−4] dendrimers,[5] dendronized polymers,[6,7] and hyper-branched polymers[8−11] with well-defined molecular structures continues to attract much attention. Molecular self-assembly is a spontaneous process in which molecules form ordered nanostructures mediated by noncovalent driving forces, typically Coulombic electrostatic interactions, van der Waals forces, $\pi-\pi$ stacking interactions, hydrogen bonding, ion-exchange, and ionic adsorption.[12−15] Combinations of solution self-assembly, interfacial self-assembly, and hybrid self-assembly processes have led to the preparation of many elaborate nanoscopic supramolecular materials, including nano- and microscale spherical micelles and vesicles, cylindrical tubules and fibers, and monolayer and multilayer arrays.[16−19] The preparation of such nanoscopic materials has been a major research area in nanoscience and -engineering. Especially, the dendritic macromolecules with specific nanostructures exhibit

Received: September 15, 2011
Accepted: March 27, 2012
Published: March 27, 2012

promising applications in fields ranging from green chemistry,[20] biochemistry,[21−28] and opto-electronics[29] to nanotechnology.[30,31]

The dendritic macromolecules possess highly branched, globular geometric shapes and an exponentially increasing number of terminal groups. Because of this, dyes, drugs, and metal ions were encapsulated by the terminal groups through ligand chelation, hydrogen bonding interaction, or electrostatic adsorption.[21,23,32] Moreover, amphiphilic dendrimers that could self-assemble in aqueous media to form hydrophobic micelle cores were applicable in encapsulation and drug delivery systems.[21,22,24,25,33] In addition, the dendritic architectures of dendrimers were also used as gates and molecular gradients for the preparation of well dispersed metal nanoparticles (NPs) in polymer solutions.[30,31] The growth of metal nanoclusters could be controlled during the formation of interdendrimer complexes, resulting in larger metal nanoclusters protected by the exterior functional groups of the dendrimers.[30,31] The stabilization and assembly of these organic/metallic nanohybrids were attributed to either the metal particles being attached to the protecting polymers or the protecting molecules covering or encapsulating the metal NPs.[30,31] In fact, the silver nanoparticles (AgNPs) have been prepared by the chemical reduction of the silver ions in linear polymer,[34,35] comb-like copolymer,[36] or dendrimer solution.[30,31] Apart from that, poly(ethylene oxide) (PEO) or polyethylene glycol (PEG) based dumbbell-shaped dendrimers have been reported for biomaterial applications.[32,37−45] However, the PEO or PEG based dumbbell-shaped dendrimers have not been used as the surfactant for the preparation of the homogeneously distributed AgNP aqueous solution. It is important to note that the preparation of the AgNPs through the chemical reduction of silver ions in micelles has not been reported.

Recently, we synthesized a series of polyurea/malonamide dendrons using 4-isocyanato-4′-(3,3-dimethyl-2,4-dioxoazetidino)diphenylmethane (IDD) as a building block.[46] Our synthetic approach toward the polyurea/malonamide dendrons, consisting of alternating addition reactions to the isocyanate and azetidine-2,4-dione groups of IDD, allowed the rapid and selective synthesis of dendrons without the need for traditional protection or activation chemistry. Such dendrons containing hydrogen bond-rich malonamide linkages along with long alkyl chains at their peripheries have served as surfactants for the surface modification of montmorillonite.[47,48] The azetidine-2,4-dione functional group of IDD undergoes ring-opening reactions with aliphatic primary amines to form malonamide linkages.[48] In order to prepare a well dispersed AgNP in micelle solution, we designed and synthesized a series of novel dumbbell-shaped dendrimers based on IDD and PEO. A two-step approach was taken to prepare these dumbbell-shaped dendrimers for the dendron synthesis, we selected IDD as the building block to prepare dendrons via a convergent route; for the synthesis of the dumbbell-shaped dendrimers, we employed hydrophilic PEO (Jeffamine ED-2003) as the coupling agent for selective ring-opening additions of azetidine-2,4-dione units. In addition, the dumbbell-shaped dendrimer based oil-in-water (O/W) micelles were prepared using a cosolvent method.[2,49] The surface tension measurements were used to evaluate the concentrations of micelles of the dumbbell-shaped dendrimers. Moreover, we employed atomic force microscopy (AFM) and transmission electron microscopy (TEM) to characterize the morphologies of the micelles derived from the dumbbell-shaped dendrimers. The morphologies obtained after the self-assembly of amphiphilic dendritic macromolecules are influenced by the chemical structures and the processing conditions (e.g., solution concentration, temperature, pH, and medium). After loading Ag^+ ions into the self-assembled supramolecules, followed by chemical reduction, we obtained a new type of organic/silver nanoparticle (AgNP) nanohybrid. We examined the effects of various relevant parameters on the sizes and shapes of these organic/AgNP nanohybrids. More importantly, better dispersion of AgNPs in micelles was achieved as compared to the ones prepared in the medium without the presence of micelles.

EXPERIMENTAL SECTION

Materials. Isobutyryl chloride, triethylamine (TEA), diethyltriamine (DETA), stearyl alcohol (C18-OH; purity = 97.0%), and PEO Jeffamine XTJ-502 (ED-2003) (M_w = 2000 kg/mol) were purchased from Sigma−Aldrich. All chemicals were purchased and used as received, unless otherwise stated. *N*,*N*-Dimethylacetamide (DMAc) was purchased from Tedia, distilled over CaH_2, and then stored over 4-Å molecular sieves. Tetrahydrofuran (THF, Tedia) was distilled over Na/benzophenone under a N_2 atmosphere prior to use. Scheme 1 displays the chemical structures of the stearyl group−functionalized IDD derivatives featuring different numbers of branched generation dendrons (from G0.5-C18 to G2.5-C18). The building block IDD and the dendrons (from G0.5-C18 to G2.5-C18) were synthesized according to previous reports.[46−48,50−54] Scheme 2 presents the synthetic route toward the amphiphilic dumbbell-shaped dendrimers. The dumbbell-shaped dendrimers (D-G0.5-C18, D-G1.5-C18, and D-G2.5-C18) were synthesized through the end-capping of ED-2003 with dendrons having different branched generations (G0.5-C18, G1.5-C18, G2.5-C18).[48,55]

Dumbbell-Shaped Dendrimer D-G0.5-C18. A solution of G0.5-C18 (0.6 g, 1.0 mmol) and ED-2003 (1.0 g, 0.5 mmol) in dry THF (15 mL) was stirred at 60 °C under a N_2 atmosphere for approximately 4 h. After cooling to room temperature, the volatiles were evaporated under reduced pressure. The crude product was purified through column chromatography (SiO_2; EtOAc/hexanes) to obtain D-G0.5-C18 as a yellowish viscous liquid (0.50 g, 35%). M_n = 4590 g mol^{-1}; PDI = 1.09. ^{1}H NMR (400 MHz, DMSO): δ 0.70−0.92 (t, 6H, CH_3), 0.93−1.50 [br, 81H, CH_2, $OC(CH_3)C$, $OCC(CH_3)$], 1.30−1.40 [s, 12H, $C(CH_3)_2$], 1.40−1.50 (m, 4H, OCH_2C), 3.0−3.7 (br, 176H, OCH_2CH_2, $OCHCH_2$, OCH_2CH), 3.78−3.94 (s, 4H, $ArCH_2Ar$), 3.95−4.15 (t, 4H, $COOCH_2$), 6.90−6.71 (d, 4H, ArH), 7.10−7.30 (d, 8H, ArH), 7.35−7.45 (d, 4H, ArH). FTIR: ν_{max} 3313 (NH), 1656 [C═O(NH)] cm^{-1}. Anal. Calcd. for $C_{173}H_{303}N_6O_{53}$: C, 62.81%; H, 9.18%; N, 2.54%; O, 25.60%. Found: C, 63.12%; H, 8.95%; N, 2.61%; O, 25.30%.

Dumbbell-Shaped Dendrimer D-G1.5-C18. D-G1.5-C18 was synthesized, using the same procedure as that described above for D-G0.5-C18, as a yellowish solid (0.81 g, 30%). M_n = 5990 g mol^{-1}; PDI = 1.04. ^{1}H NMR (400 MHz, DMSO): δ 0.78−0.91 (t, 12H, CH_3), 1.10−1.30 [br, 177 H, CH_2, $OC(CH_3)C$, $OCC(CH_3)$, $C(C_2H_6)$-CON], 1.43−1.70 (m, 8H, OCH_2C), 3.10−3.60 (br, 208 H, OCH_2CH_2, $OCHCH_2$, OCH_2CH, CONHAr), 3.70−3.90 (s, 8H, $ArCH_2Ar$), 3.90−4.10 (t, 8H, $COOCH_2$), 7.00−7.20 (d, 8H, ArH), 7.20−7.40 (d, 16H, ArH), 7.40−7.60 (d, 8H, ArH), 7.82−8.00 (b, 4H, NH), 8.40−8.60 (s, 2H, NH), 9.20−9.40 (b, 4H, NH), 9.40−9.60 (br, 4H, NH). FTIR: ν_{max} 3312 (NH), 1659 [C═O(NH)] cm^{-1}. Anal. Calcd. for $C_{293}H_{469}N_{20}O_{67}$: C, 65.89%; H, 8.79%; N, 5.25%; O, 20.10%. Found: C, 65.90%; H, 8.60%; N, 5.21%; O, 19.80%.

Dumbbell-Shaped Dendrimer D-G2.5-C18. D-G2.5-C18 was synthesized, using the same procedure as that described above for D-G0.5-C18, as a yellowish solid (0.62 g, 25%). M_n = 7453 g mol^{-1}; PDI = 1.11. ^{1}H NMR (400 MHz, DMSO): δ 0.78−0.90 (t, 24H, CH_3), 0.90−1.40 [br, 345 H, CH_2, $OC(CH_3)C$, $OCC(CH_3)$, $C(C_2H_6)$-CON], 1.40−1.63 (m, 16H, OCH_2C), 3.10−3.60 (br, 224 H, OCH_2CH_2, $OCHCH_2$, OCH_2CH, CONHAr), 3.70−3.90 (s, 28H, $ArCH_2Ar$), 3.90−4.10 (t, 16H, $COOCH_2$), 6.90−7.20 (d, 28H, ArH), 7.30−7.60 (d, 84H, ArH), 7.820−8.0 (b, 16H, NH), 8.40−8.60

Scheme 1. Synthesis of Dendrons from Building Block IDD

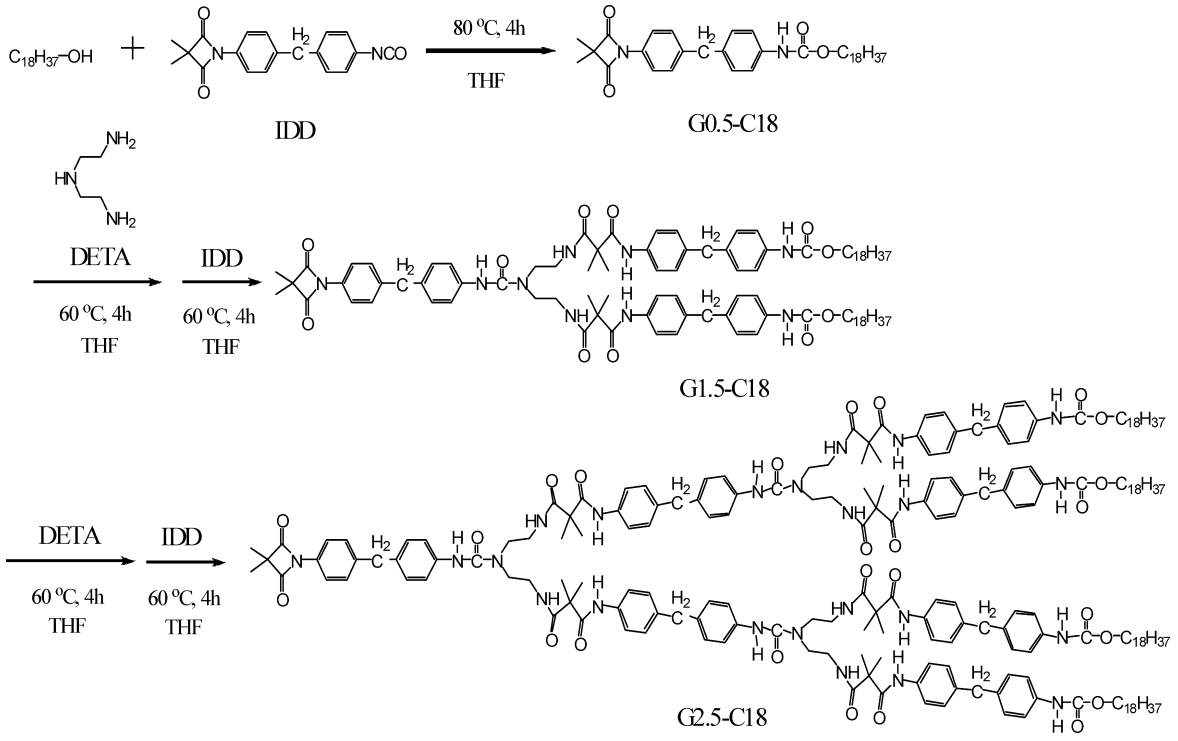

Scheme 2. Synthesis of Dumbbell-Shaped Dendrimers

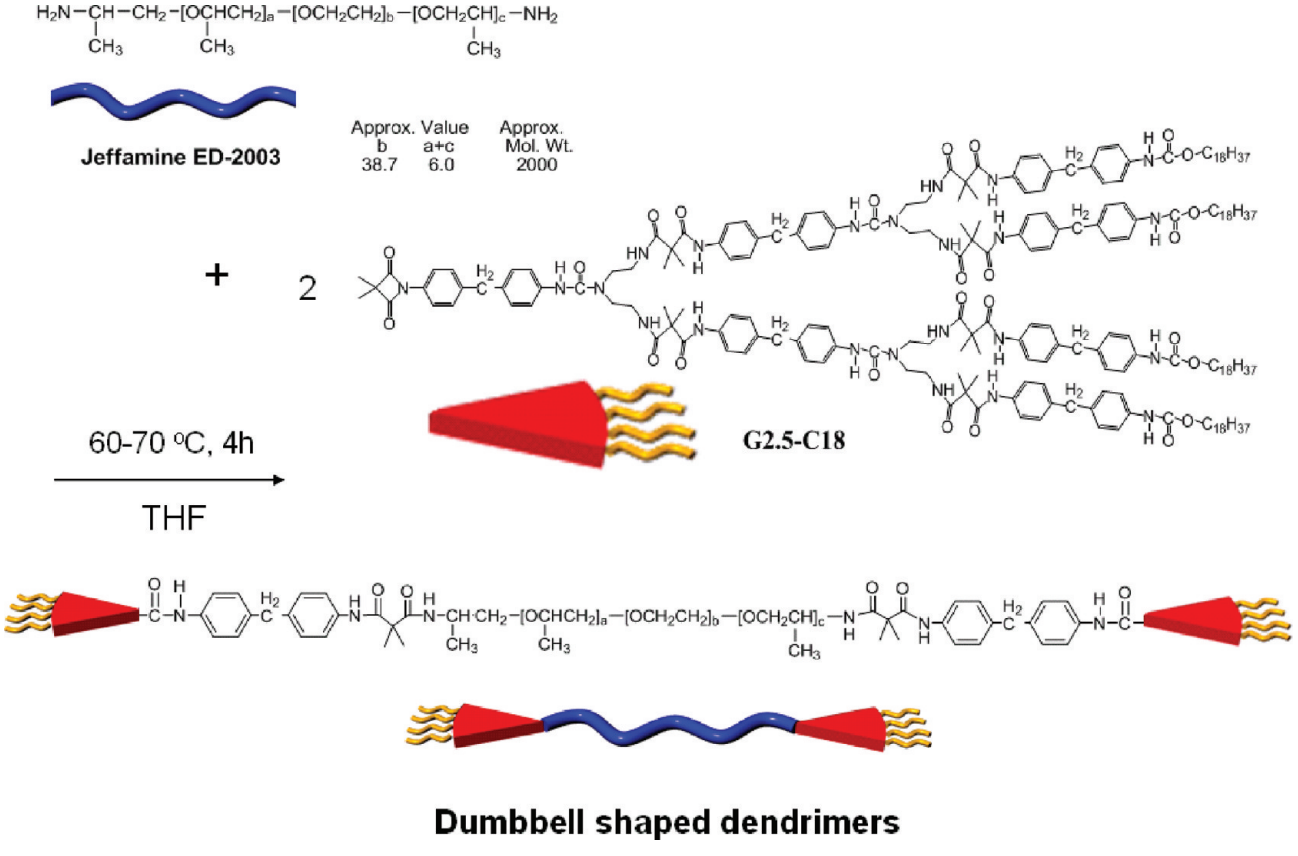

(s, 10H, NH), 9.20–9.40 (b, 20H, NH), 9.40–9.60 (b, 20H, NH). FTIR: ν_{max} 3316 (NH), 1654 [C═O(NH)] cm^{-1}. Anal. Calcd. for $C_{533}H_{831}N_{48}O_{95}$: C, 67.90%; H, 8.81%; N, 7.13%; O, 16.13%. Found: C, 67.85%; H, 8.21%; N, 7.05%; O, 16.07%.

Micelles Derived from Self-Assembly of Dendrimers. To study the self-assembly behavior of micelles based on amphiphilic dumbbell-shaped dendrimers, dendrimer based oil-in-water (O/W) micelles were prepared using a cosolvent method.[2,49] This is due to the

dx.doi.org/10.1021/am300499k | ACS Appl. Mater. Interfaces 2012, 4, 1897–1908

fact that better solubility was observed for the dendrimer in a mixed solvent (THF/water) than in the pure water.[56] For the dumbbell-shaped dendrimers (D-G0.5-C18, D-G1.5-C18, D-G2.5-C18), gelation and precipitation occurred when directly added to water. No micelle was formed in the pure water. On the other hand, a solution of a dumbbell-shaped dendrimer in THF was added slowly into vigorously stirred deionized water such that the final THF/water ratio was 1:50 (v/v). Micelles based on the dumbbell-shaped dendrimer were formed in solutions containing various contents of the dendrimer (10^{-2}, 10^{-3}, 10^{-4}, 10^{-5}, and 10^{-6} wt %). To study the self-assembly behavior of micelles on the plates of glass cells, solutions with various micelle concentrations were placed into glass cells and left to allow the solvent to evaporate, thereby inducing the self-assembly of the micelles on the glass cell plates.

AgNP Dispersal in Micelles of Dumbbell-Shaped Dendrimers. Silver nitrate ($AgNO_3$) was added [at various $AgNO_3$-to-dendrimer mole ratios (from 1 to 100 000)] to an aqueous solution containing micelles of a dumbbell-shaped dendrimer. Furthermore, four equivalents of reduction agent $NaBH_4$ were added to the solution with vigorous stirring. During the reduction process, the color of solution changed from transparent to yellowish, indicating that reduction of Ag^+ to Ag^0 was occurring in the micelle solution. The UV−vis absorption spectrum of the AgNP-dispersed micelle solution was measured to evaluate the reduction of the Ag colloid in solution. In addition, the encapsulation capacity of the AgNPs in the dumbbell-shaped dendrimer based micelles was calculated according to the literature.[11] The organic/AgNP nanohybrid solution was prepared by the reduction of the $AgNO_3$ ($AgNO_3$/D-G2.5-C18 molar ratio: 1000:1) in the dumbbell-shaped dendrimer based micelle (10^{-4} wt %, 1.34×10^{-7} M) solution. The organic/AgNP nanohybrid solution was then dialyzed against deionized water with a dialysis membrane (molecular weight cut off: 12 000−14 000 g/mol) for 24 h. The encapsulation efficiency of the AgNPs in the dumbbell-shaped dendrimer based micelles was calculated by measuring the absorption intensity of AgNPs at 389 nm before and after the dialysis of the aqueous solution of the dumbbell-shaped dendrimer based organic/AgNP nanohybrid.[11] The encapsulation efficiency of AgNPs in the dendrimer based micelles was calculated as follows:

$$\frac{I_{\text{UV absorbance after dialysis}}}{I_{\text{UV absorbance before dialysis}}} \times 100\%$$

Measurements. ^{1}H NMR spectra were recorded using a Varian Gemini-400 (400 MHz). Fourier transform infrared (FTIR) spectra were recorded using a PerkinElmer Spectrum spectrometer. Ultraviolet−visible (UV−vis) spectra were recorded using a Shimadzu UV-1240 spectrometer. Differential scanning calorimetry (DSC) and thermogravimetric analysis (TGA) were performed using a Seiko SSC-5200 apparatus operated at a heating rate of 10 °C/min under a N_2 atmosphere. The thermal degradation temperature (T_d) was taken to be the temperature at which 5% weight loss occurred. Gel permeation chromatography (GPC) was performed using a Waters chromatography system (Waters, 717 plus Autosampler), two Waters Styragel linear columns, polystyrene as the standard, and THF as the eluent. Elemental analysis was performed using a Heraeus CHN-OS Rapid Analyzer. The surface tension was measured using a FTA100 tensiometer and the pendant drop method. The critical micelle concentrations (CMCs) were the transition points obtained through extrapolation of the surfactant concentrations plotted with respect to the surface tension. X-ray diffraction (XRD) analysis was performed using a 3-kW Rigaku III diffractometer with a Cu target (λ = 1.542 Å), operated at a scanning rate of 2°/min. The d spacing of the sample was analyzed using Bragg's equation ($n\lambda = 2d \sin\theta$). Transmission electron microscopy (TEM) was performed using a Zeiss EM 902A instrument operated at 120 kV. Scanning electron microscopy (SEM) images were recorded using a Hitachi S-5200 field-emission scanning electron microscope after sputtering the films with a thin layer of Au/Pt alloy. Atomic force microscopy (AFM) images were recorded under ambient conditions using a Seiko SPI3800N Series SPA-400 operated in the tapping mode. The particle size and distribution of micelles in solution were estimated using a dynamic laser light scattering particle size analyzer (90 Plus Brookhaven Instrument Corp.) equipped with a 15 mW solid-state laser (675 nm).

RESULTS AND DISCUSSION

Scheme 1 presents the route that we used to synthesize different branched generation dendrons (from G0.5-C18 to G2.5-C18) with peripheral octadecyl chains.[46,47] The azetidine-2,4-dione functional group of IDD reacted only with aliphatic primary amino groups under the synthetic conditions employed herein. FTIR spectra of the dendrons indicated that the signals of the azetidine-2,4-dione units (1738 and 1856 cm^{-1}) disappeared, and a peak for the malonamide units appeared at 1675 cm^{-1} after the reaction between IDD and DETA. ^{1}H NMR spectra confirmed the chemical structures of the dendrons. The chemical shifts and relative intensities of the signals were in agreement with the proposed structures for these dendrons. As illustrated in Scheme 2, we synthesized the dumbbell-shaped dendrimers (dendron−coil−dendron; ABA-type) through end-capping ring-opening reactions of ED-2003 with the different branched generations of the azetidine-2,4-dione group-containing dendrons. ^{1}H NMR spectra confirmed the chemical structures of the dumbbell-shaped dendrimers (from D-G0.5-C18 to D-G2.5-C18); the chemical shifts and relative intensities of the signals (Figure 1) were in agreement with the proposed structures of these dendrimers. In addition, GPC provided valuable information confirming the purity of these dendrimers. Evolution of GPC traces (see the Supporting Information, Figure S1) shows that all dendrimers were one-peak distribution, confirming the absence of side products. Table 1 summarizes the average molecular weights of the starting ED-2003 and the dumbbell-shaped dendrimers. The molecular weights of the dumbbell-shaped dendrimers were closely related to their theoretical molecular weights, with polydispersities (PDI = 1.04−1.11) narrower than that of the starting material (ED-2003), indicating that their molecular sizes could be controlled to serve as an effective encapsulant for guest molecules.

Table 2 summarizes the TGA data of the dendrons and dumbbell-shaped dendrimers. The values of T_d (5% weight loss) of the dendrons G0.5-C18 to G2.5-C18 ranged from 250 to 278 °C. Thermal properties of the dendrons were dependent on the degree of branching and the molecular weight. Dendrons with intermediate generations (G0.5-C18, G1.5-C18, G2.5-C18) exhibited higher thermal stabilities than the dendrons with integer generation (G1.0-C18, G2.0-C18). We attribute the lower values of T_d of the dendrons G1.0-C18 and G2.0-C18 to the presence of poor thermal stability of the exposed diethylamine units in the dendrons. Moreover, the values of T_d of the dendrons increased slightly upon increasing the molecular weight. In addition, the values of T_d of the dumbbell-shaped dendrimers (from D-G0.5-C18 to D-G2.5-C18) were all in the range of 181−252 °C. It is important to note that the values of T_d of the dendrimers were lower than those of the dendrons, due to the molecular interactions between the dendritic moieties and ED-2003 segments. The molecular interaction resulted in the reduction of packing order and crystallinity of dendron based domains. Therefore, lower thermal stability was observed for the dendrimers as compared to that of the corresponding dendrons. Typically, dendrimers with higher molecular weights and higher degrees of branching dendrons exhibit higher values of T_d; we found, however, that the value of T_d of D-G2.5-C18 was lower than that of D-G1.5-C18, indicating that the high content of stearyl groups decreased the thermal stability of this dendrimer.

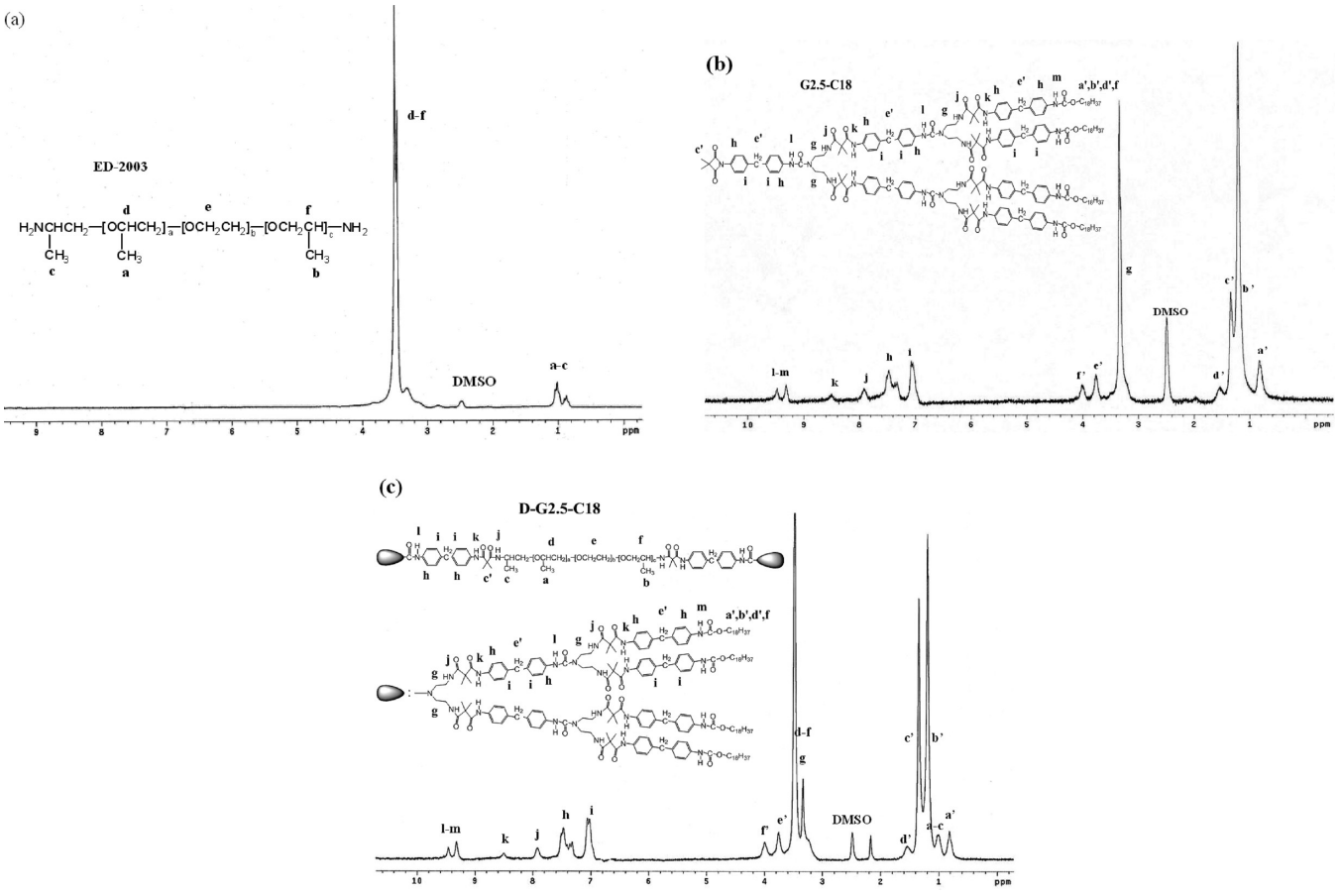

Figure 1. ^{1}H NMR spectra of (a) the ED-2003, (b) the dendron G2.5-C18, and (c) the dumbbell-shaped dendrimer D-G2.5-C18.

Table 1. Average Molecular Weights of the Dumbbell-Shaped Dendrimers[a]

sample	M_n (g/mol)	M_w (g/mol)	PDI
ED-2003	2700	3200	1.18
D-G0.5-C18	4590	5005	1.09
D-G1.5-C18	5990	6217	1.04
D-G2.5-C18	7453	8298	1.11

[a]Determined through GPC analysis with THF as eluent (calibration: polystyrene standards).

Table 2. Thermal Properties of the Dendrons and Dumbbell-Shaped Dendrimers

sample	T_d[a] (°C)	T_g[b] (°C)	T_m[b] (°C)
ED-2003	276	−65	27
G0.5-C18	272	–[c]	108
G1.0-C18	250	–	167
G1.5-C18	277	55	–
G2.0-C18	271	68	–
G2.5-C18	278	70	–
D-G0.5-C18	181	–	18/48
D-G1.5-C18	252	–	18/88
D-G2.5-C18	233	–	27/74

[a]Temperature at which 5% weight loss occurred, recorded through TGA at a heating rate of 10 °C/min. [b]Heating rate of 10 °C/min under N_2. [c]Not detectable.

Table 2 summarizes the glass transition temperatures (T_g) and melting points (T_m) of the dendrons and dendrimers.

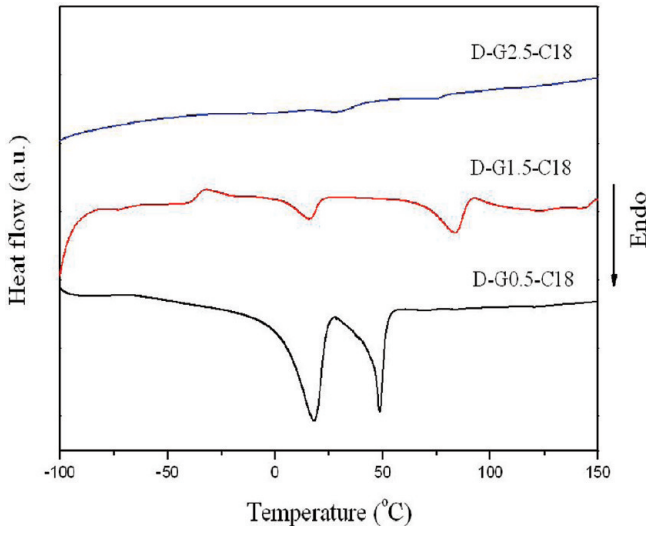

Figure 2. DSC thermograms of the dumbbell-shaped dendrimers.

According to the DSC thermograms, the dendrons G0.5-C18 and G1.0-C18 exhibited values of T_m of 108 and 167 °C, while the dendrons G1.5-C18, G2.0-C18, and G2.5-C18 possessed values of T_g of 55, 68, and 70 °C, respectively. We observed a crystalline phase for the dendron with the lower branching generation but amorphous phases for the dendrons of higher branching generation. Moreover, the value of T_g of the dendrons increased upon increasing the molecular weight and generation.[30,31] Figure 2 displays the DSC thermograms of the

dx.doi.org/10.1021/am300499k | ACS Appl. Mater. Interfaces 2012, 4, 1897−1908

dumbbell-shaped dendrimers D-G0.5-C18 to D-G2.5-C18. Because the dendrimers comprised soft (ED-2003) and hard (dendron) blocks, all of the dumbbell-shaped dendrimers displayed two values of T_m pertaining to the partial microseparation of poly(oxyalkylene) and dendron based domains, respectively. The lower value of T_m of the dendrimer was assiged to the ED-2003 based domains because the value of T_m of ED-2003 was as low as 27 °C. The values of T_m corresponding to the ED-2003 based domains in the dendrimers D-G0.5-C18, D-G1.5-C18, and D-G2.5-C18 were 18, 18, and 27 °C, respectively. The exothermic heat of T_m decreased upon increasing the branching generation of the dendrons in the dendrimers, revealing that the crystal capacity with respect to the ED-2003 based domains decreased upon the incorporation of the dendrons. The presence of the dendrons limited the molecular motion of the ED-2003 chains required for crystal organization. The chain mobility of ED-2003 would be restricted further by the presence of more highly branched generations of dendron. On the other hand, the values of T_m corresponding to the dendron based crystal domains of the dendrimers D-G0.5-C18, D-G1.5-C18, and D-G2.5-C18 were 48, 88, and 74 °C, respectively. Relative to D-G1.5-C18, the higher content of stearyl groups led to the lower value of T_m of D-G2.5-C18. In addition, as revealed in Figure 2, the exothermic heat of the melting transitions corresponding to the dendron based domains decreased upon increasing the branching generation of the dendrons. Thus, a high branching generation did not favor the formation of crystal domains of the dendrimers.

Table 3 lists the solubilities of the stearyl group-containing dendrons and dumbbell-shaped dendrimers in common organic solvents, at a concentration of 10% (w/v). Each compound exhibited good solubility in polar solvents, especially in DMAc and dimethylformamide (DMF), because of the flexible alkyl chains at the periphery of the dendrons and the polar groups of the dendrimers, including the stearyl groups, urethane, and malonamide linkages. None of the samples was soluble in MeOH, even the dendrimers containing hydrophilic poly(oxyalkylene) segments. We attribute the partial solubility of the integer-generation dendrons G1.0-C18 and G-2.0-C18 in THF and acetone to the presence of the flexible or expansible diethylamine ($CH_2CH_2NHCH_2CH_2$) linker between the aromatic-rich building blocks, allowing the conformations of G1.0-C18 and G2.0-C18 to be more linear than those of the dendrons G0.5-C18, G-1.5-C18, and G-2.5-C18. Taken together, strong $\pi-\pi$ stacking interactions between the aromatic building blocks, van der Waals forces between the long alkyl chains, and hydrogen bonding interactions between the malonamide linkages decreased the solubility of the integer-generation dendrons G1.0-C18 and G2.0-C18.

Table 3. Solubility Behavior of the Dendritic Compounds[a]

sample	THF	acetone	MeOH	DMF[b]	DMAc[b]
G0.5-C18	+ +	+ −	− −	+ +	+ +
G1.0-C18	− −	− −	− −	+ +	+ +
G1.5-C18	+ +	+ −	− −	+ +	+ +
G2.0-C18	+ −	− −	− −	+ +	+ +
G2.5-C18	+ +	+ −	− −	+ +	+ +
D-G0.5-C18	+ +	+ +	+ −	+ +	+ +
D-G1.5-C18	+ +	+ +	− −	+ +	+ +
D-G2.5-C18	+ +	+ +	− −	+ +	+ +

[a]Solubility determined from 10 mg of sample in 1 mL of solvent. + +: Soluble at room temperature. + −: Soluble after heating at 60 °C. − −: Insoluble even after heating at 60 °C. [b]DMF: Dimethylformamide; DMAc: *N*,*N*-dimethylacetamide.

To further monitor their intermolecular self-assembly behavior, the dendrons were dissolved in THF at various weight ratios (1, 10, and 20 wt %). We observed molecular aggregation and gelation only for the dendron G1.0-C18 in THF. The high branching dendron G2.0-C18 and its strong intramolecular interactions inhibited intermolecular aggregation, while the IDD units with kinked linkages inhibited the intermolecular aggregation and self-assembly of the dendrons G1.5-C18 and G2.5-C18. Therefore, gelation did not occur for the dendrons G1.5-C18, G2.0-C18, and G2.5-C18 in THF. Subsequently, we studied the molecular aggregation and gelation phenomena of the dendron G1.0-C18 in THF upon changing its concentration. As revealed in Figure 3,

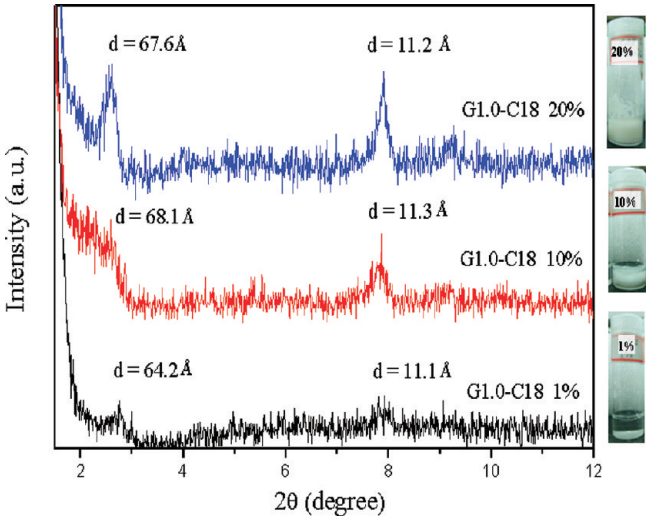

Figure 3. XRD patterns of the dried gels prepared from different weight percentages of G1.0-C18 in THF.

emulsion and gelation of the THF solution occurred when the concentration of dendron G1.0-C18 was greater than 10 wt %. We used XRD spectroscopy to further characterize the self-assembly behavior of the dendron G1.0-C18 in the gel state. Figure 3 indicates that only a high content of dendron G1.0-C18 (>5 wt %) in THF solution resulted in a gelation state. After drying the gel solution under vacuum, the XRD patterns of dried gels prepared from different concentrations of G1.0-C18 in THF revealed that the dendron molecules were integrated into regular nanostructures stabilized through strong intermolecular interactions. Two diffraction peaks with *d* spacings of 64−68 and 11 Å were evident in the spectra. Similar results have been reported for hydrogen bond-rich alkyl bis-acylurea derivatives;[57] their XRD patterns also provided evidence of 2D regular molecular packing in the organogel state. As illustrated in Figure 4, we propose that G1.0-C18 molecules self-assembled into multilayer structures, mediated by hydrogen bonds between the extended dendron molecules. The thickness of the layers of extended molecules was approximately that of the value of the *d* spacing (64−68 Å). On the other hand, we observed good solubility for the dumbbell-shaped dendrimers D-G0.5-C18 to D-G2.5-C18 in THF. Gelation did not occur for these dendrimers in THF, even though the dendron G1.0-C18 readily self-assembled into regular nanostructures through strong intermolecular interactions. Only a few dendrimers have been reported to exhibit well-defined mesophase behavior.[19] The ability of a dendrimer

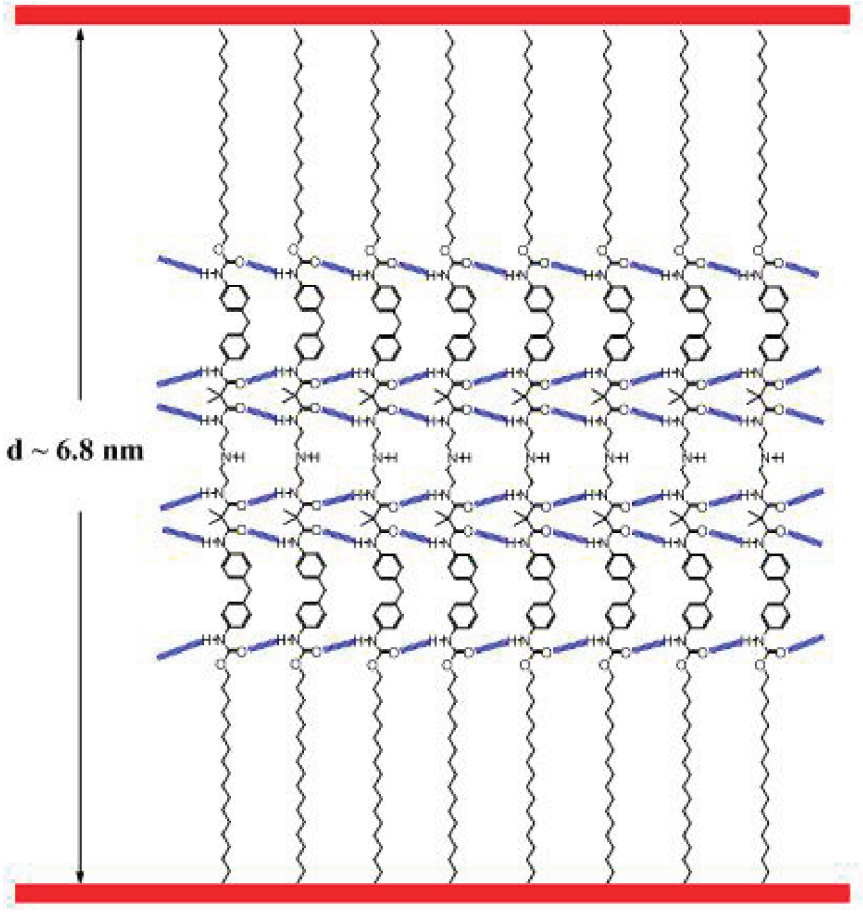

Figure 4. Schematic representation of the self-assembled lamellar structure formed from the dendron G1.0-C18.

to self-assemble is related to the shapes of its dendrons, the volume fractions of its hydrophilic and hydrophobic moieties, and the packing density of the dendritic structures.

We investigated the hydrophilic/hydrophobic balance, micellization behavior, and assembly behavior of the dendrimers with respect to their ability to decrease the surface tension of water. Figure 5 presents the concentration-dependent surface tension in the presence of the amphiphilic dumbbell-shaped dendrimers. In surface and colloid chemistry,

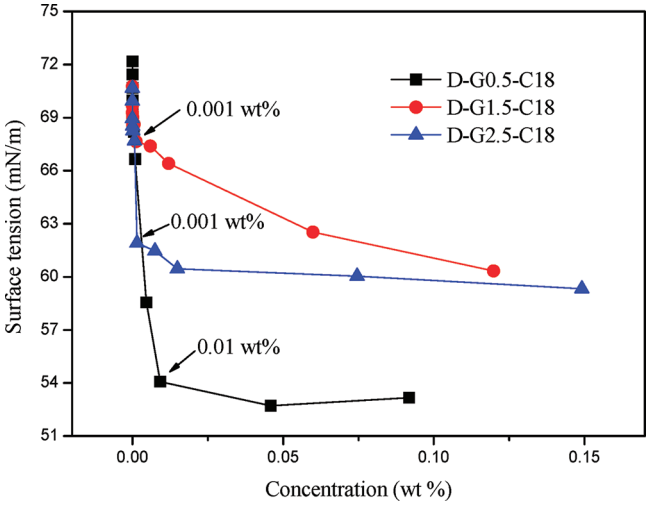

Figure 5. Surface tension as a function of concentration for the dumbbell-shaped dendrimers in aqueous solutions.

the CMC is the threshold concentration at which micellization begins; it appears as a discontinuity in the plot of the surface tension against the solution concentration. The experimental CMCs of our amphiphilic dumbbell-shaped dendrimers, determined from the turning points, ranged from 10^{-2} to 10^{-3} wt % (from ca. 2×10^{-5} to 2×10^{-6} M). The surface tension decreased from 72 to approximately 54−60 mN/m upon increasing the dendrimer content up to the CMC. The decrease in surface tension was more significant for the D-G0.5-C18 solution relative to those of the D-G1.5-C18 and D-G2.5-C18 solutions, presumably because the hydrophilicity of the dendron G0.5-C18 was greater than those of the dendrons G1.5-C18 and G2.5-C18. The hydrophilicity decreased upon increasing the contents of the building block IDD and the stearyl groups in the higher-generation dendrimers.

Compounds that form micelles are typically amphiphilic, meaning that they are soluble not only in protic solvents (e.g., water) in oil-in-water (O/W) systems but also in aprotic solvents as reverse micelles in water-in-oil (W/O) systems. A recent report suggested that spherical and relatively narrowly distributed micelles/vesicles are typically constructed through self-assembly of dendritic moieties and that they are more stable than the conventional ones obtained from linear blocks.[29,44] In aqueous media, the dumbbell-shaped dendrimers will self-assemble into O/W micelles with their hydrophobic dendrons in the core and their hydrophilic poly(oxyalkylene) segments forming loops in the corona shell, on account of the favorable hydrophilic/hydrophobic balance. Conversely, water-induced reverse micelles in nonpolar solvents (e.g., toluene)

dx.doi.org/10.1021/am300499k | ACS Appl. Mater. Interfaces 2012, 4, 1897−1908

will exhibit reverse core/shell structures relative to the micelles. Figure 6 presents graphical representations of the structures of

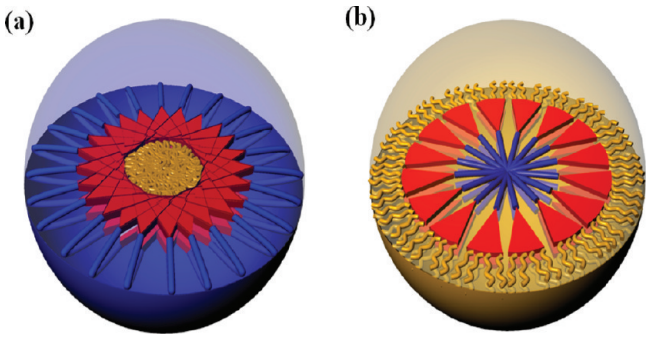

Figure 6. Schematic representations of (a) micelles and (b) reverse micelles formed from dumbbell-shaped dendrimers.

micelles and reverse micelles. Figure 7 presents SEM images of the dendrimer based micelles (10^{-4} wt %), indicating that the

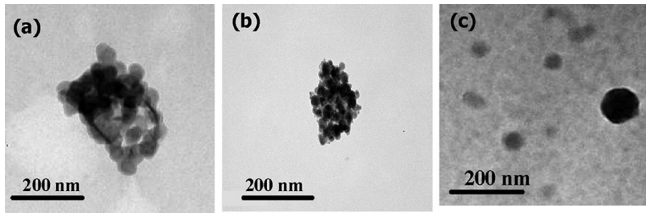

Figure 7. SEM images of micelles formed from the dendrimers (a) D-G0.5-C18, (b) D-G1.5-C18, and (c) D-G2.5-C18.

diameters of the micelles are in the range of 50−100 nm. The micelles of D-G2.5-C18 were distributed individually, while the agglomeration was observed for the micelles based on D-G0.5-C18 and D-G1.5-C18. The agglomeration of micelles implies that the micelles are not thermodynamically stable in aqueous solution. The suspension stability of micelles is related to the balance of the hydrophobicity and hydrophilicity of the dendrimer in aqueous solution. In order to investigate the dispersion of micelles in aqueous solution, the particle size and distribution of micelles were estimated using a dynamic laser light scattering particle size analyzer (as shown in Supporting Information, Figure S2). Two peak distributions of particle sizes were observed for the micelles based on D-0.5G-C18 (average size: 35 and 471 nm) and D-1.5G-C18 (average size: 60 and 614 nm), while the average particle size of D-2.5G-C18 based micelles with monodispersity was about 157 nm. The result is congruent with the observation of SEM images. The agglomeration of micelles led to two different particle size distributions for the D-0.5G-C18 and D-1.5G-C18 based micelles. On the other hand, the particle size peak distribution with monodispersity indicates that the D-2.5G-C18 based micelles exhibited excellent dispersion in aqueous solution. In addition, the particle size of the micelle was dependent on the volume fractions and molecular interactions of its hydrophilic and hydrophobic moieties.[1,8,9,12,19,29,47] The average particle size of D-2.5G-C18 based micelles is larger than those of the micelles based on D-0.5G-C18 and D-1.5G-C18. The average particle size and distribution of dendrimer based micelles in aqueous solution play an important role for the preparation of organic/metallic nanohybrids.

The nano- to micrometer-scale secondary structures of aggregates (e.g., micelles, vesicles, fibers, ribbons, sheets) are dependent on the molecular structure, concentration, solvent solubility, and other solution variables (e.g., pH, ionic strength). Figure 8 presents a possible mechanism for the formation of

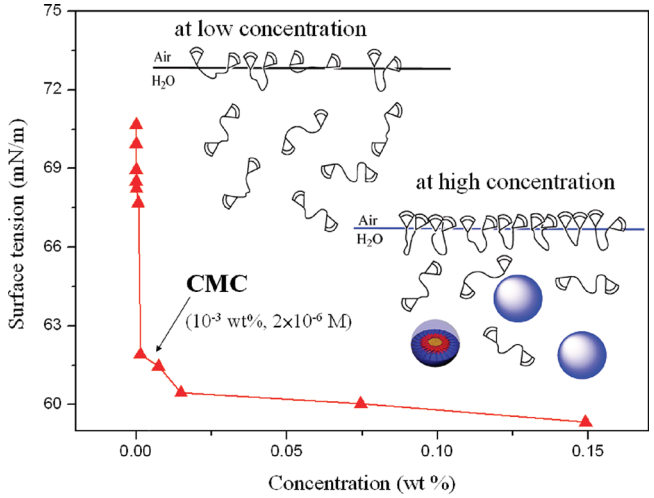

Figure 8. Surface tension as a function of concentration for D-G2.5-C18 in aqueous solution and schematic representation of micelle formation.

micelles from the amphiphilic dendrimer D-G2.5-C18 in aqueous solution. When the concentration of D-G2.5-C18 was less than CMC (ca. 10^{-3} wt %), the molecules of D-G2.5-C18 adsorbed and aggregated at the surface of the solution, thereby decreasing the surface tension; indeed, the surface tension decreased from 72 to approximately 60 mN/m upon increasing the concentration of D-G2.5-C18 in the aqueous solution up to CMC. Moreover, the molecules of D-G2.5-C18 could simply dissipate individually at the concentration below CMC and formed small aggregates or partially sank from the interface into the bulk of the aqueous solution when the concentration was close to CMC, at which point the adsorption of D-G2.5-C18 was saturated at the surface of the solution.[58] By definition, micelles will begin to form in a solution at CMC, the structures of which will depend on the structures of the amphiphilic molecules. When the concentration is greater than the CMC, these molecules spontaneously aggregate to form clusters (micelles), which result from physical interactions among the amphiphilic molecules rather than covalent bonding.

To further study the formation of micelles in aqueous solution, we prepared adsorbed D-G2.5-C18 substrates by dipping a glass plate into its solution for 24 h and then allowing the water to evaporate under ambient conditions. Figure 9a−d presents SEM images of the adsorbed substrates prepared from various concentrations of D-G2.5-C18 in aqueous solutions. When the concentration of D-G2.5-C18 in the aqueous solution was much less than CMC, only a few micelles formed in solution; the molecules of D-G2.5-C18 aggregated to form a colloidal material on the substrate (Figure 9a). When the concentration of D-G2.5-C18 increased to near CMC (10^{-4} wt %), symmetrical deformed (donut-shaped) micelles (outer diameter: 50−150 nm) formed on the glass plate (Figure 9b). It has been reported that the micelles with about 100 nm size were formed by the amphiphilic dumbbell-shaped dendrimers[59] and hyper-branched polymers.[8] We attribute the deformation

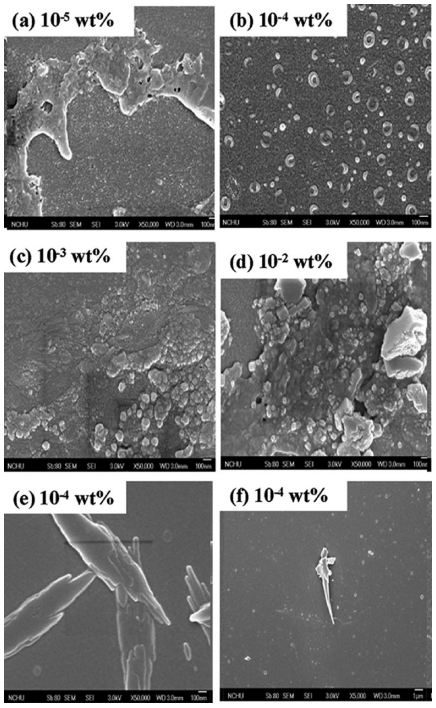

Figure 9. SEM images of micelles on glass plates, prepared from various concentrations of the dumbbell-shaped dendrimers (a–d) D-G2.5-C18, (e) D-G0.5-C18, and (f) D-G1.5-C18.

of the micelles to the collapse of hemispherical micelles on the glass plate upon evaporation of the water. Figure 10 provided a schematic illustration of the formation of D-G2.5-C18 based spherical micelles and their assembly on the substrate. Because of hydrophobic/hydrophilic balance, the center of each hemispherical micelle comprised mainly dendritic fragments (C18-dendron periphery). The formation of the donut shape was due to the lack of interpenetration and entanglement of the dendritic fragments in the middle of the hemispherical micelles.[60] As a result, donut-shaped micelles were formed on the substrate. This observation is consistent with the formation of micelles in aqueous solution. Furthermore, the micelle content increased with increasing concentration of D-G2.5-C18 in solution; as a result, aggregation of the micelles occurred on the substrate. As revealed in Figure 9c,d, greater degrees of adsorption of the micelle based clusters occurred on the substrate for aqueous solutions containing higher concentrations of D-G2.5-C18 (10^{-2} and 10^{-3} wt %, respectively). In contrast, the dendrimers D-G0.5-C18 (Figure 9e) and D-G1.5-C18 (Figure 9f) did not form donut-shaped micelles on the glass plates. Bulk solid particles were formed on the glass plate for the dendrimers D-G0.5-C18 and D-G1.5-C18. The formation of bulk solid particles was presumably attributed to the high molecular interaction and agglomeration of the dendrimers on the glass plate.

Recently, poly(ethylene glycol)s of various chain lengths have been reported to play greater roles as stabilizers than as reducing agents for Ag^+ ions.[61] The favorable complexation of ethoxy (CH_2CH_2O) groups with Ag^+ ions is well established.[62,63] In each ethoxy-containing micelle colloid, we postulated that the hydrophobic dendrons were sequestered and solvated with THF in the core. Apart from that, the hydrophilic poly(oxyalkylene) loops were extended away from the center and bound to water molecules through hydrogen bonds. Therefore, we expected the corona exterior of the micelles, presenting poly(oxyalkylene) segment functionalities, to be capable of chelating Ag^+ ions and mediating their in situ reduction to form AgNPs. The long poly(oxyalkylene) loops extending into the aqueous phase and complexing the Ag^+ ions would provide suspension and steric stabilization to efficiently prevent the resulting AgNPs from collision and flocculation.

In aqueous solutions containing D-G2.5-C18 based micelles (10^{-4} wt %, 1.34×10^{-7} M), we used $NaBH_4$ as a reducing agent to transform various molar ratios of $AgNO_3$ into zero-valence AgNPs. During the reduction process, we confirmed the formation of micelle-stabilized AgNPs by observing color changes from colorless to yellowish, without precipitation. The yellow color of the colloidal sample (inset to Figure 11) is indicative of the presence of spherical AgNPs and the formation of Ag nanoclusters in solution. Furthermore, by varying the molar ratio of $AgNO_3$ to D-G2.5-C18 and monitoring the maximum UV–vis absorption of the solution, we established the reaction profile and optimal conditions for the transformation. Figure 11 presents the UV–vis spectra of the micelle-stabilized AgNPs prepared at various $AgNO_3$/D-G2.5-C18 ratios. The maximum absorption appeared at a wavelength of 389 nm, corresponding to the dipole resonance of Ag nanospheres.[56,64] The intensity of the absorption peak increased upon increasing the molar ratio of $AgNO_3$ to D-G2.5-C18. The absorption reached its maximum intensity

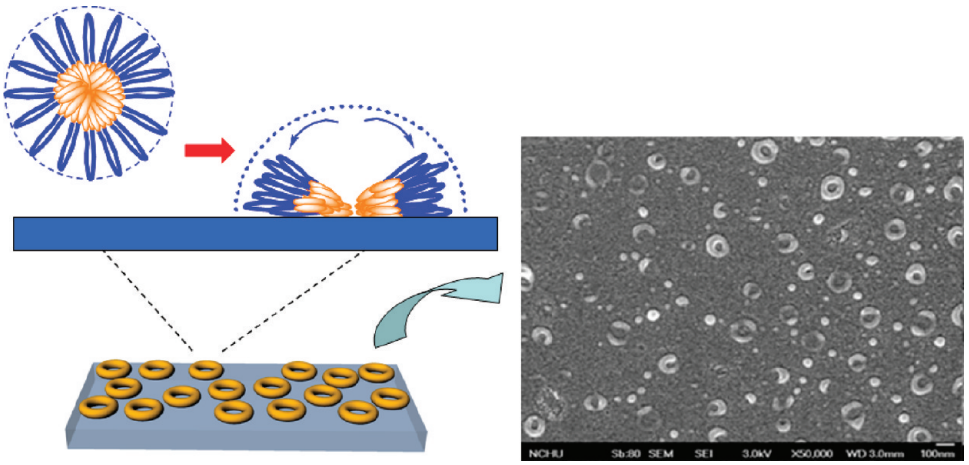

Figure 10. Schematic representation of spherical micelles assembled from the dendrimer D-G2.5-C18 on a substrate.

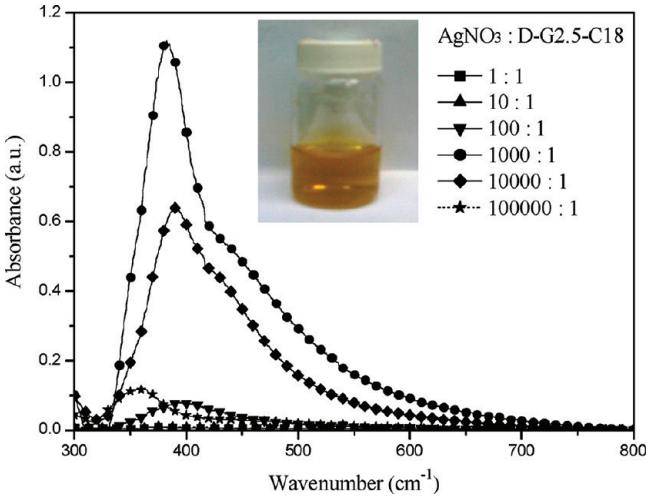

Figure 11. UV−vis spectra of micelle-stabilized AgNPs prepared at various $AgNO_3$/D-G2.5-C18 ratios; inset: photograph of the sample prepared at a $AgNO_3$/D-G2.5-C18 ratio of 1000:1.

when the $AgNO_3$/D-G2.5-C18 molar ratio was 1000:1, gradually decreasing thereafter up to a ratio of 10^5 because of the lower loading of D-G2.5-C18. In addition, the colloid based on the reduced $AgNO_3$/D-G2.5-C18 (molar ratio: 1000:1) system remained well dispersed in the aqueous solution. No aggregation of the Ag nanocomposite occurred in the colloid (inset to Figure 11).

Figure 12 provides a schematic representation of the self-assembly, with controllable particle size, of the AgNPs in the D-G2.5-C18 based micelles. After the addition of an appropriate amount of reducing agent, the AgNPs that formed were positioned initially between the extended poly(oxyalkylene) loops, but they gradually diffused into the dendron-rich core. SEM images reveal that the micelle particles had an average diameter of approximately 50−100 nm; TEM indicates that the average diameter of the spherical AgNPs was approximately 10−30 nm. Figure 13 presents TEM micrographs of the ED-2003-stabilized and dendrimer (D-G0.5-C18 to D-G2.5-C18)-stabilized AgNPs. The AgNPs aggregated into large particles (average diameter: 20 nm) when we used ED-2003 as the template (Figure 13a); their dispersion was not uniform. We observed similar behavior for the D-G0.5-C18- and D-G1.5-C18-stabilized AgNPs (Figure 13b,c, respectively). We attribute the aggregation of these AgNPs to the agglomeration of micelles in the aqueous solutions containing D-G0.5-C18 and D-G1.5-C18. In contrast, the AgNPs obtained after reduction of the $AgNO_3$/D-G2.5-C18 micelles (Figure 13d) featured a homogeneous dispersion in the form of round nanoclusters; the average diameter of these AgNPs was much lower than 10 nm, while the average diameter of the round nanoclusters was approximately 50−200 nm. Almost all of the AgNPs were spherical. These results indicate that micelles of the amphiphilic dumbbell-shaped dendrimer D-G2.5-C18 were the more effective templates for hosting nanoclusters and stabilizing AgNPs to form unique organic/metallic nanohybrids. In addition to the distribution of AgNPs in the organic/AgNP nanohybrid, the encapsulation efficiency of the AgNPs in the micelles of dumbbell-shaped dendrimer was also investigated. The absorption intensity of AgNPs at 389 nm was reduced after the dialysis of the aqueous solution of the organic/AgNP nanohybrid (see the Supporting Information, Figure S3). According to the absorption intensity of AgNPs in the organic/AgNP nanohybrid, the encapsulation efficiencies of AgNPs were about 69.04, 56.48, and 54.07% for the micelles of D-G0.5-C18, D-G1.5-C18, and D-G2.5-C18, respectively. The encapsulation efficiency of AgNPs was closely related to the steric effect of the dendritic structure and the number of reduction groups of amines and oxyethylenes.[31,34,36]

CONCLUSION

We have synthesized structurally symmetrical dendrimers (D-G0.5-C18 to D-G2.5-C18) featuring dendron−coil−dendron structures comprising an identical poly(oxyalkylene) middle block and different generation dendrons with peripheral octadecyl alkyl

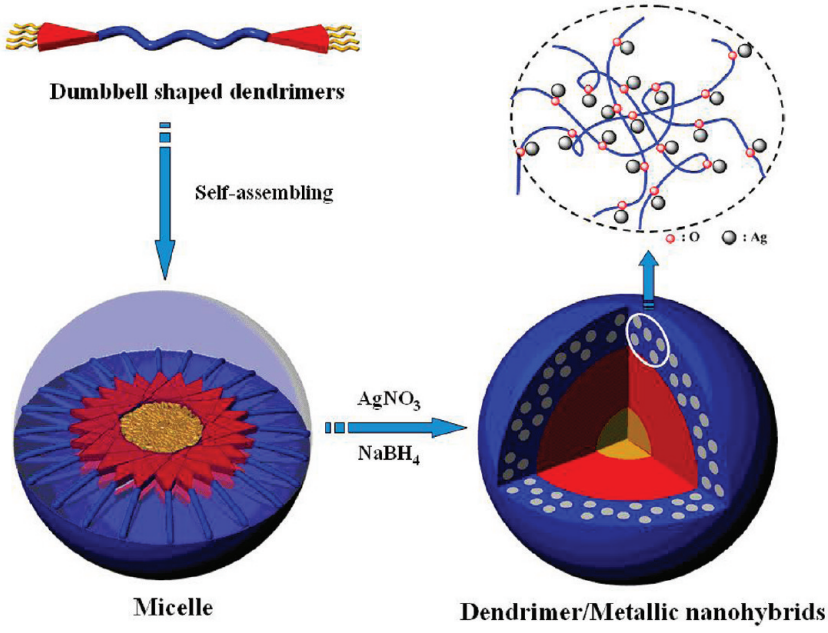

Figure 12. Schematic representation of micelle-stabilized AgNPs.

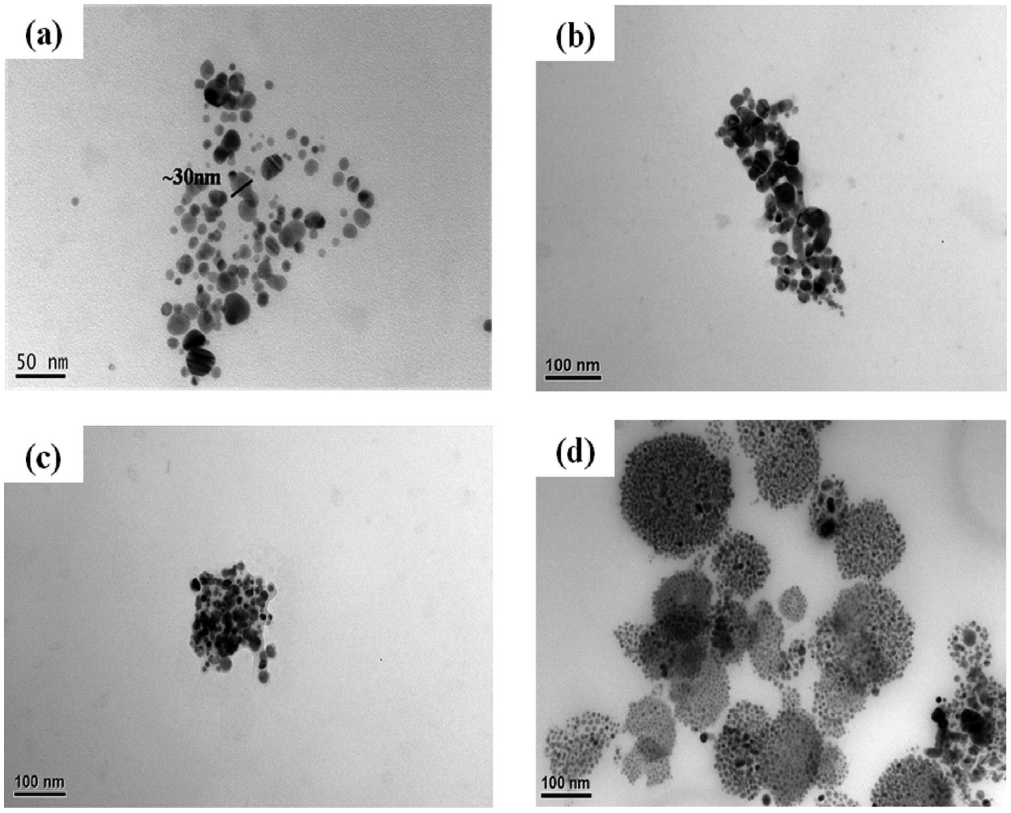

Figure 13. TEM micrographs of the micelle-stabilized AgNPs prepared using (a) ED-2003, (b) D-G0.5-C18, (c) D-G1.5-C18, and (d) D-G2.5-C18 as templates (10^{-4} wt % in aqueous solution).

chains. The thermal stability and solubility of these dendrimers was closely related to the generation of the dendrons. We observed a crystalline phase for the dendron with the lowest branching generation; the other dendrons with higher branching generations exhibited amorphous phases. A combination of strong $\pi-\pi$ stacking between the aromatic building blocks, van der Waals forces between the long alkyl chains, and hydrogen bonding interactions between the malonamide linkages resulted in the lower solubility of the integer-generation dendrons. A correlation between the structure and surface tension revealed that the amphiphilic dumbbell-shaped dendrimer D-G2.5-C18 could self-assemble into micelles or large particles depending on its concentration in water. In aqueous media, the dumbbell-shaped dendrimers self-assembled into micelles with their hydrophobic dendrons in the core and their hydrophilic poly(oxyalkylene) segments forming the loops in the corona shell, on account of favorable hydrophilic/hydrophobic balance. SEM images revealed that the dendrimer D-G2.5-C18 was robust at forming micelles in aqueous media; these micelles, which featured hydrophobic cores surrounded by hydrophilic exterior poly(oxyalkylene) loops, were effective at stabilizing and assembling AgNPs to form organic/metallic nanohybrids. After the reduction of $AgNO_3$, the AgNPs were distributed homogeneously in the dendrimer micelle–stabilized AgNP nanoclusters. High encapsulation efficiency of AgNPs was also observed for the dumbbell-shaped dendrimer based micelles.

■ ASSOCIATED CONTENT

Ⓢ Supporting Information

Figures of GPC traces of the dumbbell-shaped dendrimers and starting material PEO ED-2003, the particle size of the dendrimer based micelles in aqueous solution, and the absorption intensity of AgNPs before and after dialysis of the aqueous solution of the dumbbell-shaped dendrimer based organic/AgNP nanohybrid. This material is available free of charge via the Internet at http://pubs.acs.org.

■ AUTHOR INFORMATION

Corresponding Author

*Tel.: +886-2-33665884. Fax: +886-2-33665237. E-mail: rhl@nchu.edu.tw (R.-H.L.); rujong@ntu.edu.tw (R.-J.J.).

Notes

The authors declare no competing financial interest.

■ ACKNOWLEDGMENTS

We thank the National Science Council of Taiwan for financial support.

■ REFERENCES

(1) Estroff, L. A.; Hamilton, A. D. *Chem. Rev.* **2004**, *104*, 1201.
(2) Zhang, W.; Shi, L.; An, Y.; Shen, X.; Guo, Y.; Gao, L.; Liu, Z.; He, B. *Langmuir* **2003**, *19*, 6026.
(3) Di Cola, E.; Lefebvre, C.; Deffieux, A.; Narayanan, T.; Borsali, R. *Soft Matter* **2009**, *5*, 1081.
(4) Riess, G. *Prog. Polym. Sci.* **2003**, *28*, 1107.
(5) Percec, V.; Won, B. C.; Peterca, M.; Heiney, P. A. *J. Am. Chem. Soc.* **2007**, *129*, 11265.
(6) Zhang, A. F.; Shu, L. J.; Bo, Z. S.; Schlüter, A. D. *Macromol. Chem. Phys.* **2003**, *204*, 328.
(7) Kurzbach, D.; Kattnig, D. R.; Zhang, B.; Schlüter, A. D.; Hinderberger, D. *J. Phys. Chem. Lett.* **2011**, *2*, 1583.
(8) Zhou, Y.; Yan, D. *Chem. Commun.* **2009**, 1172.
(9) Zeng, F.; Zimmerman, S. C. *Chem. Rev.* **1997**, *97*, 1681.

(10) Zhao, Y. H.; Xu, Y. Y.; Zhu, B. K. *Solid State Ionics* **2009**, *180*, 1517.
(11) Zhang, L.; Hu, C. H.; Cheng, S. X.; Zhuo, R. X. *Colloids Surf., B: Biointerfaces* **2010**, *79*, 427.
(12) Whitesides, G. M.; Grzybowski, B. A. *Science* **2002**, *295*, 2418.
(13) Ho, R. H.; Chiang, Y. W.; Lin, S. S.; Chen, C. K. *Prog. Polym. Sci.* **2011**, *36*, 376.
(14) Dawn, A.; Shiroki, T.; Haraguchi, S.; Tamaru, S. I.; Shinkai, S. *Chem. Asian J.* **2011**, *6*, 266.
(15) Zhang, X.; Wang, C. *Chem. Soc. Rev.* **2011**, *40*, 94.
(16) Kunitake, T.; Okahata, Y.; Shimomura, M.; Yasunami, S. I.; Takarabe, K. *J. Am. Chem. Soc.* **1981**, *103*, 5401.
(17) Herr, D. J. C. *J. Mater. Res.* **2011**, *26*, 122.
(18) Hamley, I. W. *Soft Matter* **2011**, *7*, 4122.
(19) Cho, B. K.; Jain, A.; Gruner, S. M.; Wiesner, U. *Chem. Commun.* **2005**, 2143.
(20) Simonyan, A.; Gitsov, I. *Langmuir* **2008**, *24*, 11431.
(21) Aulenta, F.; Hayes, W.; Rannard, S. *Eur. Polym. J.* **2003**, *39*, 1741.
(22) Liu, M.; Kono, K.; Fréchet, M. J. *J. Controlled Release* **2000**, *65*, 121.
(23) Stiriba, S. E.; Frey, H; Haag, R. *Angew. Chem., Int. Ed.* **2002**, *41*, 1329.
(24) Weinhart, M.; Groger, D.; Enders, S.; Riese, S. B.; Dernedde, J.; Kainthan, R. K.; Brooks, D. E.; Haag, R. *Macromol. Biosci.* **2011**, *11*, 1088.
(25) Papp, I.; Sieben, C.; Sission, A. L.; Kostka, J.; Bottcher, C.; Ludwig, K.; Herrmann, A.; Hang, R. *ChemBioChem* **2011**, *12*, 887.
(26) Gillies, E. R.; Frechet, J. M. J. *J. Am. Chem. Soc.* **2002**, *124*, 14137.
(27) Ihre, H. R.; Jesus, O. L. P. D; Szoka, F. C.; Frechet, J. M. J. *Bioconjugate Chem.* **2002**, *13*, 443.
(28) Gitsov, I.; Hamzik, J.; Ryan, J.; Simonyan, A.; Nakas, J. P.; Omori, S.; Krastanov, A.; Cohen, T.; Tanenbaum, S. W. *Biomacromolecules* **2008**, *9*, 804.
(29) Xiong, W.; Wang, H.; Han, Y. *Macromol. Rapid Commun.* **2010**, *31*, 1886.
(30) Sun, X.; Dong, S.; Wang, E. *Macromolecules* **2004**, *37*, 7105.
(31) Kuo, P. L.; Chen, W. F. *J. Phys. Chem. B* **2003**, *107*, 11267.
(32) Chapman, T. M.; Hillyer, G. L.; Mahan, E. J.; Shaffer, K. A. *J. Am. Chem. Soc.* **1994**, *116*, 11195.
(33) Bronstein, L. M.; Shifrina, Z. B. *Chem. Rev.* **2011**, *111*, 5301.
(34) Dong, R. X.; Tsai, W. C.; Lin, J. J. *Eur. Polym. J.* **2011**, *47*, 1383.
(35) Chen, D. H.; Huang, Y. W. *J. Colloid Interface Sci.* **2002**, *255*, 299.
(36) Hsu, Y. C.; Chen, Y. M.; Lin, W. L.; Lan, Y. F.; Chan, Y. N.; Lin, J. J. *J. Colloid Interface Sci.* **2010**, *352*, 81.
(37) Gitsov, I.; Wooley, K. L.; Fréchet, J. M. J. *Angew. Chem., Int. Ed. Engl.* **1992**, *31*, 1200.
(38) Gitsov, I.; Lambrych, K. R.; Remnant, V. A.; Pracitto, R. *J. Polym. Sci., Part A: Polym. Chem.* **2000**, *38*, 2711.
(39) Gitsov, I.; Simonyan, A.; Vladimirov, N. G. *J. Polym. Sci., Part A: Polym. Chem.* **2007**, *45*, 5136.
(40) Froimowicz, P.; Gandini, A.; Strumia, M. *Tetrahedron Lett.* **2005**, *46*, 2653.
(41) Yu, D.; Vladimirov, N.; Frechet, J. M. J. *Macromolecules* **1999**, *32*, 5186.
(42) Gitsov, I.; Wooley, K. L.; Hawker, C. J.; Ivanova, P. T.; Frechet, J. M. J. *Macromolecules* **1993**, *26*, 5621.
(43) Gitsov, I.; Hamzik, J.; Ryan, J.; Simonyan, A.; Nakas, J. P.; Omori, S.; Krastanov, A.; Cohen, T.; Tanenbaum, S. W. *Biomacromolecules* **2008**, *9*, 804.
(44) Gitsov, I.; Fréchet, J. M. J. *Macromolecules* **1993**, *26*, 6536.
(45) Cho, B. K.; Jain, A.; Gruner, S. M.; Wiesner, U. *Chem. Commun.* **2005**, 2143.
(46) Chen, C. P.; Dai, S. A.; Chang, H. L.; Su, W. C.; Jeng, R. J. *J. Polym. Sci., Part A: Polym. Chem.* **2005**, *43*, 682.
(47) Tsai, C. C.; Juang, T. Y.; Dai, S. A.; Wu, T. M.; Su, W. C.; Liu, Y. L.; Jeng, R. J. *J. Mater. Chem.* **2006**, *16*, 2056.
(48) Dai, S. A.; Juang, T. Y.; Chen, C. P.; Chang, H. Y.; Kuo, W. J.; Su, W. C.; Jeng, R. J. *J. Appl. Polym. Sci.* **2007**, *103*, 3591.
(49) Ge, Z.; Chen, D.; Zhang, J.; Rao, J.; Yin, J.; Wang, D.; Wan, X.; Shi, W.; Liu, S. *J. Polym. Sci., Part A: Polym. Chem.* **2007**, *45*, 1432.
(50) Kuo, M. C.; Tung, Y. C.; Yeh, C. L.; Chang, H. Y.; Jeng, R. J.; Dai, S. A. *Macromolecules* **2008**, *41*, 9637.
(51) Liu, J. K.; Shau, S. M.; Juang, T. Y.; Chang, C. C.; Dai, S. A.; Su, W. C.; Lin, C. H.; Jeng, R. J. *J. Appl. Polym. Sci.* **2011**, *120*, 2411.
(52) Chang, H. L.; Chao, T. Y.; Yang, C. C.; Dai, S. A.; Jeng, R. J. *Eur. Polym. J.* **2007**, *43*, 3988.
(53) Juang, T. Y.; Tsai, C. C.; Wu, T. M.; Dai, S. A.; Chen, C. P.; Lin, J. J.; Liu, Y. L.; Jeng, R. J. *Nanotechnology* **2007**, *18*, 205606.
(54) Tsai, C. C.; Chang, C. C.; Yu, C. S.; Dai, S. A.; Wu, T. M.; Su, W. C.; Chen, C. N.; Chen, F. M. C.; Jeng, R. J. *J. Mater. Chem.* **2009**, *19*, 8484.
(55) Gitsov, I. *J. Polym. Sci., Part A: Polym. Chem.* **2008**, *46*, 5295.
(56) Pastoriza-Santos, I.; Liz-Marzán, L. M. *Nano Lett.* **2002**, *2*, 903.
(57) Davis, R.; Berger, R.; Zentel, R. *Adv. Mater.* **2007**, *19*, 3878.
(58) Fréchet, J. M. J.; Gitsov, I.; Monteil, T.; Rochat, S.; Sassi, J. F.; Vergelati, C.; Yu, D. *Chem. Mater.* **1999**, *11*, 1267.
(59) Chang, Y.; Park, C.; Kim, K. T.; Kim, C. *Langmuir* **2005**, *21*, 4334.
(60) Yang, M.; Wang, W.; Yuan, F.; Zhang, X.; Li, J.; Liang, F.; He, B.; Minch, B.; Wegner, G. *J. Am. Chem. Soc.* **2005**, *127*, 15107.
(61) Kim, C. K.; Kim, C. K.; Lee, B. S.; Won, J.; Kim, H. S.; Kang, Y. S. *J. Phys. Chem., Part A: Polym. Chem.* **2001**, *105*, 9024.
(62) Kima, M.; Byun, J. W.; Shin, D. S.; Lee, Y. S. *Mater. Res. Bull.* **2009**, *44*, 334.
(63) Bouzide, A.; Sauvé, G. *Org. Lett.* **2002**, *4*, 2329.
(64) Jin, R.; Cao, Y. W.; Mirkin, C. A.; Kelly, K. L.; Schatz, G. C.; Zheng, J. G. *Science* **2001**, *294*, 1901.